Environ Earth Sci (2016) 75:362
DOI 10.1007/s12665-015-4929-y

ORIGINAL ARTICLE

Cu(II) adsorption from aqueous solution using red mud activated by chemical and thermal treatment

Fabiano T. da Conceição[1] · Beatriz C. Pichinelli[2] · Mariana S. G. Silva[2] · Rodrigo Braga Moruzzi[1] · Amauri Antonio Menegário[3] · Maria Lucia Pereira Antunes[4]

Received: 24 February 2015 / Accepted: 20 August 2015 / Published online: 22 February 2016

Abstract Brazil is the third-largest producer of aluminium, with the red mud generated during the extraction of aluminium from bauxite through the Bayer process. The red mud has been studied for use as an adsorbent for removing of elements/compounds from wastewater and/or contaminated soil. However, there are several compounds and treatments that were not tested yet. In this study, the Cu(II) adsorption potential for natural red mud (NRN) and red mud activated by thermal treatment at 400 °C (TRM) and chemical treatment with hydrochloric acid (HCl) at 0.05 mol L^{-1} (CRM1) and calcium nitrate [$Ca(NO_3)_2$] 0.1 mol L^{-1} (CRM2) was evaluated using adsorption isotherms obtained by the Langmuir and Freundlich models. The NRM and TRM presented Cu(II) adsorptions of ca. 100 % in aqueous solution with lower concentrations of the metal (0.5 and 1.0 mmol 25 mL^{-1}). The Langmuir isotherm was more appropriate to describe the phenomenon of Cu(II) removal using NRM, TRM, CRM1 and CRM2, with the thermally activated red mud presenting the highest adsorption capacity at 2.08 mmol g^{-1} for Cu(II). Thus, these results indicate that TRM has the potential for use in applications that treat effluents and/or contaminated soil from industrial activity.

✉ Fabiano T. da Conceição
ftomazini@rc.unesp.br

[1] Instituto de Geociências e Ciências Exatas (IGCE), UNESP, Universidade Estadual Paulista, Avenida 24-A, No. 1515, Bela Vista, Rio Claro, São Paulo CEP 13506-900, Brazil

[2] Faculdade de Engenharia de Bauru (FEB), UNESP, Universidade Estadual Paulista, Bauru, Brazil

[3] Centro de Estudos Ambientais (CEA), UNESP, Universidade Estadual Paulista, Rio Claro, Brazil

[4] UNESP, Universidade Estadual Paulista, Campus Experimental de Sorocaba, Sorocaba, Brazil

Keywords Aluminium production · Red mud · Cu(II) adsorption · Isotherms models

Introduction

Pollution changes the physical, chemical and biological characteristics of many hydrospheric, atmospheric, biospheric and pedospheric components by interfering with their quality and preventing their use for human activities. Depending on the industry, metals can be released in the environment as emissions, effluents or solid waste. Although certain metals are biogenetic and essential for living organisms, the majority are accumulative poisons when they are ingested at higher concentrations than the recommended values because they undergo biomagnification and have the potential to cause mutagenic, teratogenic and carcinogenic effects or even death (Aguiar et al. 2002; Von Sperling 2005); therefore, removing metals are very essential.

The main anthropogenic sources of the metal copper are mining and casting, burning coal as an energy source and incinerating waste. Depending on the particle size, compounds that contain copper undergo dry disposal or are carried by rainwater. The major routes of exposure are inhalation, food and water ingestion, dermal contact and oral administration. The ingestion of copper salts causes vomiting, lethargy, acute haemolytic anaemia, kidney and liver damage, and even death (Cetesb 2012).

Several methods have been used for the removal of metals from industrial effluents and contaminated soils, including precipitation, membrane filtration, ion exchange, electrolysis and adsorption by activated carbon (Nadaroglu et al. 2010). However, the economic and technical criteria are not always achieved. Hence, low-cost methods for environmental remediation and industrial effluent

treatment that do not change the characteristics of the environment must be developed.

Currently, the most frequently used technique for metal removal in the remediation of contaminated soils or treatment of industrial effluents is adsorption because it is more efficient and easy to use and has a greater variety of possible low-cost adsorbents. Different industrial wastes are used as adsorbents for the removal of metals from contaminated soils or industrial effluents, and red mud, which is a by-product of the processing of bauxite, is highlighted (Nadaroglu et al. 2010).

Red mud is generated in large quantities from the extraction of aluminium from bauxite through the Bayer process, and it is disposed in locations referred to as "disposal lagoons". The amount of red mud generated by such activities is up to twice the amount of alumina produced. Hence, its disposal requires an extensive area, which contributes to the increased of cost of the aluminium production process. Red mud is not classified as hazardous waste (EPA 2014), but it may cause the contamination of water springs, produce caustic rains, and harm plants and animals in the region around the disposal lagoon.

To reuse this industrial waste, red mud in its natural form or chemically or thermally treated can be used as a low-cost metal adsorbent. Studies have evaluated the adsorption of copper by natural red mud (Nadaroglu et al. 2010) and red mud chemically treated with hydrochloric acid (Apak et al. 1998a; Agrawal et al. 2004) or calcium sulphate (Lopez et al. 1998). However, no studies have been produced in Brazil using natural red mud or with different thermal or chemical activations for the adsorption of Cu(II) from aqueous solutions.

Thus, the purpose of this study was to evaluate the Cu(II) adsorption potential for red mud activated with different treatments from aqueous solution and the results were modelling by means of Langmuir and Freundlich isotherms. The natural red mud (NRM) was activated by thermal treatment at 400 °C (TRM) and by chemical treatment with hydrochloric acid (HCl) at 0.05 mol L^{-1} (CRM1) and calcium nitrate [$Ca(NO_3)_2$] 0.1 mol L^{-1} (CRM2), and then characterised by different techniques, such as pH, electrical conductivity, ion exchange capacity, specific surface area and mineralogical composition.

Experimental method

Sampling and activation

The red mud samples were collected from an aluminium production company located in the city of Alumínio, near Sorocaba City in the countryside of São Paulo State, Brazil. To initiate the activations, all of the NRM samples were crushed in a porcelain crucible and passed through a 150 μm.

For the thermal treatment, the samples were placed in porcelain crucibles and heated in a muffle oven at 400 °C (TRM), where they remained for a period of 2 h. For the activation with HCl, the NRM samples were mixed with 0.05 mol L^{-1} HCl (CRM1) at a ratio of 1:25 (g of red mud per mL of HCl). The beakers with the mixture were agitated for 2 h, and they were then left to rest for the decantation of activated mud. Then, the supernatant was removed and distilled water was added to the remaining red mud; this process was repeated once more to wash the mud. The remaining mud was dried throughout the night in the oven at a temperature of 60 °C. Another chemical treatment for NRM was performed with 0.1 mol L^{-1} $Ca(NO_3)_2$ (CRM2), and the same activation procedures described above for HCl 0.05 mol L^{-1} were followed.

Characterisation of natural red mud and red mud with different activations

For the grain-size analysis of the NRM samples, the procedures described by Klute (1986) were followed. The pH values and electrical conductivity were determined at a ratio of 1 g of red mud to 25 mL of distilled and deionised water. A YSI 556 MultiProbe System (Yellow Springs, OH, USA) was calibrated to characterise highly pure standards at pH 4.00 (4.00 ± 0.01 at 25± 0.2 °C) and 7.00 (7.00 ± 0.01 at 25 ± 0.2 °C) and with a standard KCl solution (1.0 mmol L^{-1}) of known conductivity for 147 μS cm^{-1} at 25 °C. The ion exchange capacity (IEC; $mmol_{(+)}$ kg^{-1}) was obtained with Eq. 1 (Claessen 1997):

$$\mathrm{IEC} = [8 \times (M_{\mathrm{EDTA}} \times V_{\mathrm{b}}) - (M_{\mathrm{EDTA}} \times V_{\mathrm{am}})] \times 10^{6}, \quad (1)$$

where M_{EDTA} = the molar concentration of EDTA (mol L^{-1}); V_{b} = the EDTA volume used for the titration of the blank (L); V_{am} = the EDTA used for the titration of the sample (L).

The NRM samples and red mud with different activations were characterised according to their specific surface area using nitrogen adsorption curves. The samples were degasified at 200 °C overnight before analysis. To obtain the nitrogen adsorption isotherms, a Micromeritics ASAP Tristar 3000 analyser (Norcross, GA, USA) was operated at −196 °C. The specific surface areas and grain sizes were calculated with the mathematical model by Brunauer, Emmett and Teller (Brunauer et al. 1938). The mineralogical analyses were performed by X-ray diffraction in a Siemens D5000 diffractometer (Erlangen, Germany) with Cu radiation (WL = 1.542 Å) and a Ni filter. The goniometer speed was defined as 3° min^{-1} with an exposure time of 1 s for every 0.05°. An additional method was used for the mineralogical visualisation and identification

that included scanning electron microscopy coupled with energy dispersive spectroscopy (SEM–EDS) using an SEM Field Emission Gun (JSM 6330F, JEOL, Boston, MA, USA). This technique identified the mineral phases that occurred at percentages of less than 5 %, which is a limiting factor for X-ray diffraction.

Adsorption studies

The test samples were prepared according to the procedures of Santona et al. (2006). Eight solutions containing different concentrations of hydrated copper(II) nitrate ($Cu(NO_3)_2{\cdot}3H_2O$) were prepared: 0.5, 1.0, 1.5, 2.0, 2.5, 3.0, 3.5 and 4.0 mmol 25 mL^{-1}. One gram of NRM was added to each of the solutions, and the same procedures were performed for the TRM, CRM1 and CRM2. All of the adsorption tests were performed under conditions of controlled pH during all experiment time, varying from 5.0 to 5.5. The Cu(II) concentrations were quantified by inductively coupled plasma optical emission spectrometry (ICP-OES) at the Centre for Environmental Studies (Centro de Estudos Ambientais, CEA) of the State University of São Paulo (Universidade Estadual Paulista, UNESP) at Rio Claro. The amount of Cu(II) retained by the adsorbent q_e (mmol g^{-1}) was calculated by the mass balance ratio presented in Eq. 2. The adsorption percentage (%A) of Cu(II) was obtained with Eq. 3. All of the Cu(II) analyses used for the adsorption tests were performed in triplicate and the average values are reported.

$$q_e = \frac{(C_o - C_e) \times V}{m}, \quad (2)$$

$$\%A = \frac{(C_o - C_e)}{C_o} \times 100, \quad (3)$$

where C_0 and C_e = the initial and equilibrium concentration of Cu(II), respectively (mmol 25 mL^{-1}); V = the volume of the solution (25 mL); m = the adsorbent mass (1 g).

Results and discussion

Characterisation of natural red mud and red mud with different activations

The results obtained for the grain-size fractions of NRM display variations in the grain size of 49, 42 and 9 % for clay, silt and sand, respectively. According to the Guide for the Texture Classes and Guide for Grouping of Texture Classes (Manual Técnico de Pedologia 2007), the red mud samples belong to the "silty clay" class. The results obtained for the parameters pH, electrical conductivity, IEC and specific surface area characterised for the NRM, TRM, CRM1 and CRM2 are presented in Table 1.

Table 1 Characterization of NRM, TRM, CRM1 and CRM2

Parameter	NRM	TRM	CRM1	CRM2
pH	10.3	10.9	8.7	7.9
Electrical conductivity (μS cm^{-1})	3700	1600	247	137
IEC ($mmol_{(+)}$ kg^{-1})	109	101	112	110
Specific surface area (m^2 g^{-1})	31	56	79	40
Pore diameter (nm)	3–4	1–4	3–4	3–4

The NRM presents an alkaline pH (10.3) and high electrical conductivity (3700 μS cm^{-1}). After the activations with 0.05 mol L^{-1} HCl and 0.1 mol L^{-1} $Ca(NO_3)_2$, the pH and electrical conductivity values were reduced to 8.7 and 7.9 and 247 and 137 μS cm^{-1}, respectively. The thermal treatment increased the pH values from 10.3 to 10.9 and decreased the electrical conductivity to 1600 μS cm^{-1}. Regarding the IEC, the highest result was obtained for CRM1 (112 $mmol_{(+)}$ kg^{-1}). The CRM2 presented the second highest IEC (110 $mmol_{(+)}$ kg^{-1}), followed by the NRM (109 $mmol_{(+)}$ kg^{-1}) and TRM (101 $mmol_{(+)}$ kg^{-1}). The observed values approached the values obtained by Santona et al. (2006), which were 106.5 and 120.6 $mmol_{(+)}$ kg^{-1} for the NRM and 98.2 $mmol_{(+)}$ kg^{-1} for mud treated with HCl.

The CRM1 presented a larger specific surface area (79 m^2 g^{-1}), and the NRM presented the smallest value of this parameter (31 m^2 g^{-1}). The results obtained for the TRM and CRM2 were 56 and 40 m^2 g^{-1}, respectively. Hence, the activations caused an increase in specific surface area relative to natural mud. The pore diameter for the NRM, CRM1 and CRM2 was between 3 and 4 nm and classified as mesopores. The TRM presented diameters varying from 1 to 4 nm and was classified as micro to mesopores. Natural red mud and red mud with different treatments were composed of particles of different sizes and shapes (Fig. 1), with particles ranging from lower than 1 μm up to higher than 10 μm of diameter. In addition, the different activations did not change the mineral morphology.

Figure 2 illustrates the XRD patterns obtained for the NRM and with different activations. The NRM presented the following mineralogy: muscovite ($KAl_2Si_3AlO_{10}(OH)_2$), goethite (FeOOH), calcite ($CaCO_3$), sodalite ($Na_8Al_6Si_6O_{24}Cl_2$), gibbsite ($Al(OH)_3$), quartz (SiO_2) and rutile (TiO_2). CRM1 and CRM2 contained the same minerals as NRM, whereas the peaks corresponding to goethite and gibbsite were not observed for the TRM, however, the peak for hematite (Fe_2O_3) was verified. According to Antunes et al. (2012), thermal treatment is responsible for changing of goethite to hematite at 234 °C ($FeO(OH) \rightarrow Fe_2O_3$) and

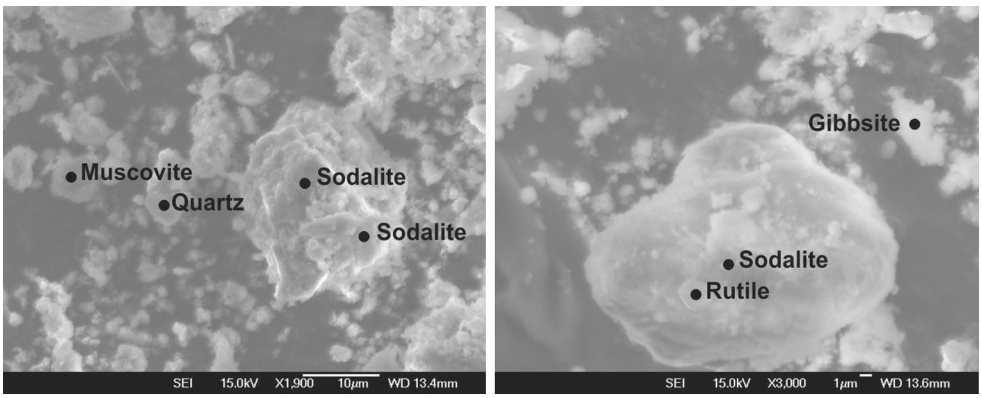

Fig. 1 SEM-EDS of NRM

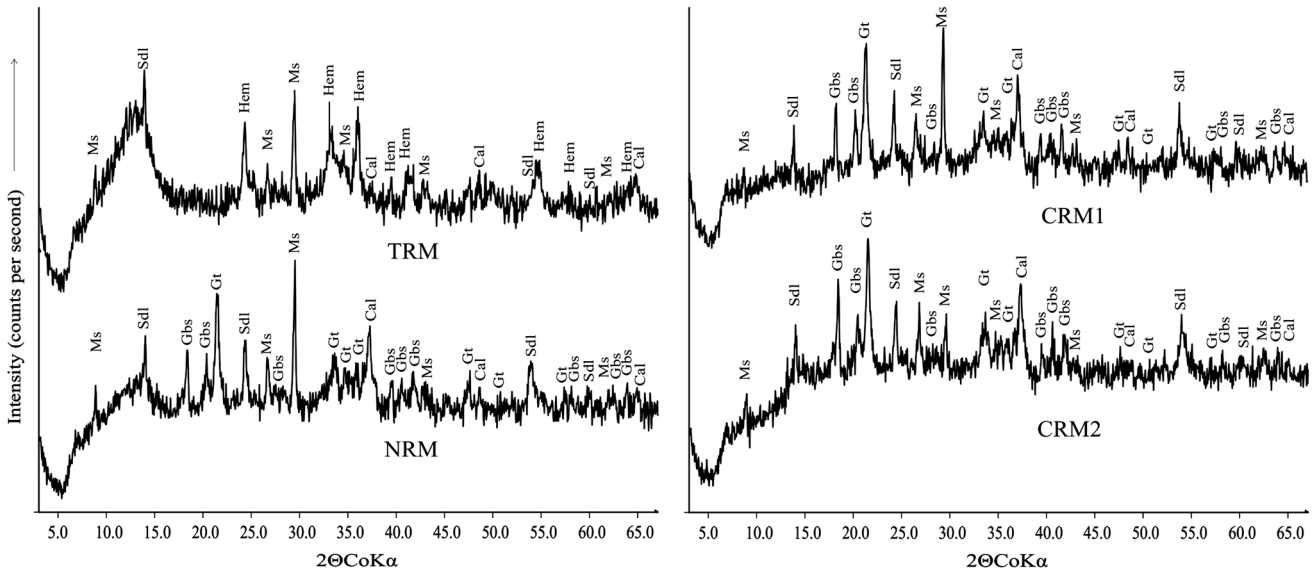

Fig. 2 XRD patterns of NRM, TRM, CRM1 and CRM2. *Sdl* sodalite, *Gds* gibbsite, *Gt* goethite, *Kln* kaolinite, *Hem* hematite, *Qtz* quartz, *Cal* calcite

gibbsite to alumina at 272 °C ($Al(OH)_3 \rightarrow Al(OH)_{(S)} + -H_2O \rightarrow Al_2O_3 + H_2O$). The increment of alumina in the red mud, which has a specific surface area higher than the original aluminium hydroxide, promotes the increase in the specific surface area of TRM.

Percentage of Cu(II) adsorption

The percentages of Cu(II) adsorption obtained for NRM and with different activations are presented in Fig. 3a, and the ratio C_0 versus q_e is presented in Fig. 3b. The total amount of Cu(II) in the aqueous solutions was high enough to satisfy the cationic exchange capacity of NRM and all of its activations. The removal of Cu(II) by all of the red muds was higher than their respective IEC. In addition, there was no precipitation of Cu(II) during the adsorption experiments due to pH of solution, which varying from 5.0 to 5.5.

The analysis of Cu(II) removal demonstrated a different percentage of removal for each red mud according to the following increasing order: TRM, NRM, CRM2 and CRM1. The relative standard deviation for all samples was lower than 4 %. The NRM presented Cu(II) adsorption percentages varying from 44.8 to 99.8 % as a function of the initial concentration (C_0). The TRM was the material that presented the highest percentage of Cu(II) adsorption, with values between 54.2 and 99.9 %. Additionally, the NRM and TRM present values approaching 100 % Cu(II) removal for lower concentrations (0.5–1.0 mmol 25 mL^{-1}). After chemical activation, the CRM1 and CRM2 presented values of Cu(II) removal varying from 39.4 to 79.4 % and 45.8 to 93.9 %, respectively, which represented the lowest percentages for the removal of this metal.

Sodalite is a calcium and sodium tectosilicate of open porous structure and can be considered a material with

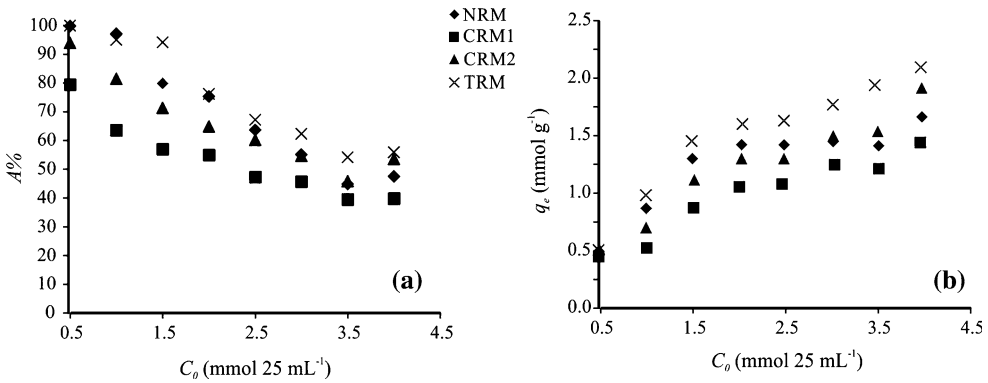

Fig. 3 The percentages of Cu(II) adsorption (**a**) and the ratio C_0 versus q_e (**b**) for NRM, TRM, CRM1 and CRM2

zeolite-type properties. This crystalline phase was found in all red mud samples examined in this study. This mineral appears to be the main phase related to the adsorption capacity of red mud because all of the mud samples presented high adsorption capacity for this metal. Because the equilibrium pH of the aqueous solutions used in the experiments was lower than the point of zero charge, with value ca. 9.0 to red mud as reported by Antunes et al. (2012), a positive charge density was observed in its lattice, which does not favours the adsorption of metals on sodalite surface.

However, sodalite possesses β-cages (with aperture diameter of 0.22 ηm) made up of six-membered rings in its frameworks, which are negatively charged due to substitution of Si^{4+} by Al^{3+} (Mon et al. 2005). Therefore, Cu(II) can be exchanged with cations presents in the β-cages, which are responsible for balancing the charge of the structural framework of sodalite. Thus, due to NRM, TRM, CRM1 and CRM2 used in this study contains large amounts of sodalite, they present a high capacity for removing Cu(II).

The chemical treatment with hydrochloric acid dissolves a portion of the sodalite, approximately 9 % according to Santona et al. (2006), and almost all of the muscovite found in NRM, which can be observed in Fig. 2. Although there is an increase in the specific surface area for CRM1, this adsorbent presents the lowest percentage of Cu(II) removal, which reinforce the idea that sodalite is an important mineral for the adsorption process of Cu(II) by NRM and at different activations.

However, there are other minerals in addition to sodalite that contribute to the adsorption process. When NRM is thermally activated at 400 °C, there is an increase in its specific surface area (from 31 to 51 m^2 g^{-1}), decrease in the pores diameters and transformation of goethite and gibbsite into hematite and alumina, respectively. The presence of Al and Fe oxides allows the adsorption of Cu(II) due to positively charged surfaces through the formation of specific inner-sphere bonds (Santona et al. 2006). Therefore, TRM was the adsorbent that presented the greatest percentage of Cu(II) removal for all of the concentrations used in the experiments.

Cu(II) adsorption isotherms

Adsorption isotherms are obtained by mathematical equations used to describe adsorption. These isotherms represent the amount of an adsorbed element relative to the remaining concentration in the equilibrium solution. The most frequently used models to describe adsorptions are those proposed by Freundlich and Langmuir.

The model by Freundlich (Eq. 4) considers the non-uniformity of real surfaces and describes the ionic adsorption within certain limits of concentration; however, this model presents difficulties for higher values, and its main disadvantage is that it is not based on physical models (Di Bernardo and Dantas 2005; Valladares et al. 1998).

$$q_e = K_F \times C_e^{\frac{1}{n}}, \quad (4)$$

where K_F = the adsorption capacity (mmol g^{-1}) (L $mmol^{-1})^{1/n}$; $1/n$ = the adsorption intensity.

The Langmuir model (Eq. 5) is based on adsorption occurring at uniform sites with a monolayer cover and ionic affinity regardless of the amount of adsorbed material. Its main disadvantage is the use of its linear form where the maximum adsorption is not properly estimated (Di Bernardo and Dantas 2005; Valladares et al. 1998).

$$q_e = \frac{(q_m \times K_L \times C_e)}{(1 + K_L \times C_e)}, \quad (5)$$

where q_m = the maximum adsorption capacity (mmol g^{-1}); K_L = the adsorption equilibrium constant.

Isotherms of Cu(II) adsorption created with the observed values and values obtained by the Langmuir and Freundlich models for NRM and at different activations are found in Fig. 4. The results of these adjustments are presented in Table 2. The experimental data provided a good fit for both models, which can be observed in Fig. 4 and

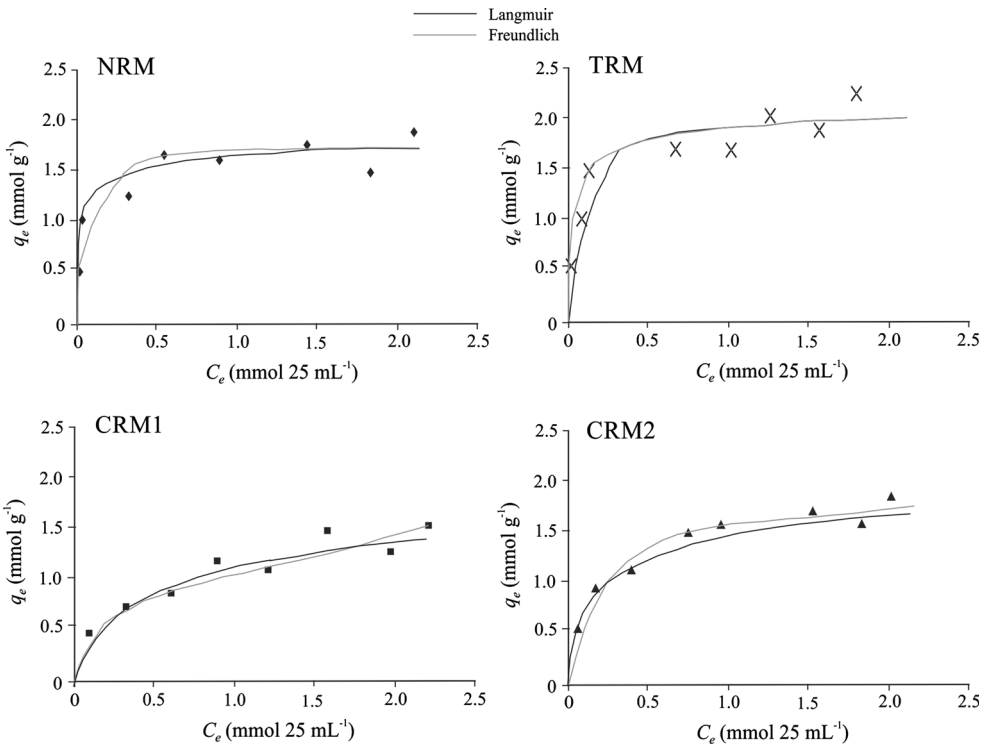

Fig. 4 Adsorption isotherms of Cu(II) by NRM, TRM, CRM1 and CRM2 using the Langmuir and Freundlich adsorption models

Table 2 Parameters of adsorption using Langmuir and Freundlich models for the NRM, TRM, CRM1 and CRM2

	NRM	TRM	CRM1	CRM2
Langmuir parameters				
q_m (mmol g^{-1})	1.76	2.08	1.84	2.01
K_L	17.20	13.09	3.83	1.69
R^2	0.97	0.97	0.92	0.95
Freundlich parameters				
K_F [(mmol g^{-1}) (L mmol^{-1})$^{-1/n}$]	1.60	1.85	1.05	1.50
$1/n$	0.15	0.16	0.43	0.32
R^2	0.95	0.95	0.95	0.96

Table 2, and the relatedness coefficients presented values that were high and similar.

The highest value for maximum Cu(II) adsorption capacity was obtained for the TRM (2.08 mmol g^{-1}), followed by CRM2 (2.01 mmol g^{-1}), CRM1 (1.84 mmol g^{-1}) and NRM (1.76 mmol g^{-1}). The highest value associated with TRM can be attributed to presence of sodalite and transformation of goethite and gibbsite into hematite and alumina, respectively, increase in specific surface area and decrease in pore diameter. The parameters obtained by the Freundlich model complemented the results obtained by the Langmuir model. The highest K_F value [in (mmol g^{-1}) (L mmol^{-1})$^{1/n}$] was obtained for the TRM (1.85), thus confirming its highest adsorption capacity, being this fact associated with presence of hematite in TRM. The lowest K_F value was 1.05, which was obtained for the CRM1. For the NRM and CRM2, the K_F values were 1.60 and 1.50, respectively.

The results obtained for the q_m (mmol g^{-1}) of Cu(II) for NRM and at different activations were higher than those found in other studies for natural red mud (and 0.08 mmol g^{-1}—Nadaroglu et al. 2010), red mud treated with HCl. i.e. 1.05 mmol g^{-1} (Apak et al. 1998a) and 0.04 mmol g^{-1} (Agrawal et al. 2004) and aggregated prepared using red mud and $CaSO_4$ (1.02 mmol g^{-1}—Apak et al. 1998b). Furthermore, the observed q_m values for all activations were higher than the value obtained for red mud activated with calcium sulphate (0.31 mmol g^{-1}) (López et al. 1998).

The q_m values presented in this study are even higher than those found for other adsorbents, such as coal mining waste (0.004 mmol g^{-1}—Geremias et al. 2012), clay (0.007–0.032 mmol g^{-1}—Aragão et al. 2013), bentonite (0.039 mmol g^{-1}—Tito et al. 2008; 0.50 mmol g^{-1}—Anna et al. 2015), moriche palm activated charcoal (0.007 mmol g^{-1}—Pinto et al. 2012), chitosan capsules (0.098 mmol g^{-1}—Valentini et al. 2000), water treatment residues (0.089 mmol g^{-1}—Castaldi et al. 2015), cotton boll (0.18 mmol g^{-1}—Ozsoy and Kumbur 2006), xanthate-modified magnetic chitosan (0.54 mmol g^{-1}—Zhua et al. 2012), porous geopolymeric spheres (0.82 mmol g^{-1}—Ge et al. 2015) and expanded perlite (0.14 mmol g^{-1}—Saria et al. 2007).

Conclusion

In this study, the characterisation of red mud and adsorption of Cu(II) by the NRM and at different chemical (HCl 0.05 mol L^{-1}—CRM1; and $Ca(NO_3)_2$ 0.1 mol L^{-1}—CRM2) and thermal (400 °C) activations (TRM) were evaluated. The heat treatment of red mud at 400 °C increases the specific surface area due to chancing of goethite to hematite and gibbsite to alumina and decreases the pores particles. The highest percent removal of Cu(II) was observed by the NRM and TRM at pH values ranging from 5.0 to 5.5. The removal of Cu(II) in aqueous solution obeys the Langmuir model, with maximum adsorption capacity related to TRM (2.08 mmol g^{-1}). The q_m values presented in this study are even higher than those found for natural or activated red mud and other adsorbents. Thus, this study suggests that the natural red mud or red mud with different treatments, especially the TRM, have the potential for use in the treatment of effluents and/or contaminated soil from industrial activity.

Acknowledgments The authors acknowledge the Fundação de Amparo à Pesquisa do Estado de São Paulo (FAPESP, Process No. 2009/02374-0), Conselho Nacional de Desenvolvimento Científico e Tecnológico (CNPq, Process No. 480555/2009-5) and Companhia Brasileira de Alumínio (CBA).

Compliance with ethical standards

Conflict of interest The authors declare that they have no conflict of interest.

References

Agrawal A, Sahu KK, Pandey BD (2004) A comparative adsorption study of copper on various industrial solid wastes. AIChE J 50:2430–2438

Aguiar MRMP, Novaes AC, Guarino AWS (2002) Remoção de metais pesados de efluentes industriais por aluminossilicatos. Quim Nova 25:1145–1154

Anna B, Kleopas M, Constantine S, Anestis F, Maria B (2015) Adsorption of Cd(II), Cu(II), Ni(II) and Pb(II) onto natural bentonite: study in mono- and multi-metal systems. Environ Earth Sci 73:5435–5444

Antunes MLP, Couperthwaite SJ, Conceição FT, Jesus CPC, Kiyohara PK, Coelho ACV, Frost RL (2012) Red mud from Brazil: thermal behavior and physical properties. Ind Eng Chem Res 51:775–779

Apak R, Guclu K, Turgut MH (1998a) Modeling of copper(II), cadmium(II) and lead(II) adsorption on red mud. J Colloids Interf Sci 203:122–130

Apak R, Tütem E, Hügül M, Hizal J (1998b) Heavy metal cation retention by unconventional sorbents (red muds and fly ashes). Water Res 32:430–440

Aragão DM, Arguelho MLPM, Alves JPH, Prado CMO (2013) Estudo Comparativo da Adsorção de Pb(II), Cd(II) e Cu(II) em Argila Natural Caulinítica e Contendo Montmorilonita. Orbital Electron J Chem 5:157–163

Brunauer S, Emmett PH, Teller E (1938) Adsorption of gases in multimolecular layers. J Am Chem Soc 60:309–319

Castaldi P, Silvetti M, Garau G, Demurtas D, Deiana S (2015) Copper(II) and lead(II) removal from aqueous solution by water treatment residues. J Hazard Mater 283:140–147

Cetesb (2012) Ficha de Informação Toxicológica. Cobre. http://www.cetesb.sp.gov.br/userfiles/file/laboratorios/fit/cobre.pdf. Accessed 12 Sept 2012

Claessen MEC (org.) (1997) Manual de métodos de análise de solo, 2nd edn. EMBRAPA-CNPS, Rio de Janeiro

Di Bernardo L, Dantas AD (2005) Métodos e técnicas de tratamento de água—2 V, 2nd edn. RiMa, São Carlos

EPA (2014) Environmental Protection Agency, Electronic code of federal regulations. Title 40, Part 261, Sect 4 (b) (7) (ii) (c). http://ecfr.gpoaccess.gov. Accessed 25 Aug 2014

Ge Y, Cui X, Kong Y, Li Z, He Y, Zhou Q (2015) Porous geopolymeric spheres for removal of Cu(II) from aqueous solution: synthesis and evaluation. J Hazard Mater 283:244–251

Geremias R, Laus R, Fávere VT, Pedrosa RC (2012) Adsorção de íons Cu(II), Mn(II), Zn(II) e Fe(III), utilizando rejeito de mineração de carvão como adsorvente. Rev Bras Cienc Amb 25:48–59

Klute A (1986) Methods of soil analysis. Part 1: Physical and mineralogical methods. In: Gee GG, Bauder JW (eds) Particle size analysis, 2nd edn. ASA and SSSA, Madison

Lopez E, Soto B, Arias M, Nunez A, Rubinos D, Barral MT (1998) Adsorbent properties of red mud and its use for wastewater treatment. Water Res 32:1314–1322

Manual Técnico de Pedologia (2007) Fundação Instituto Brasileiro de Geografia e Estatística. Departamento de Recursos Naturais e Estudos Ambientais; Oliveira VA, coord; IBGE Rio de Janeiro

Mon J, Deng Y, Flury M, Harsh JB (2005) Cesium incorporation and diffusion in cancrinite, sodalite, zeolite, and allophane. Microporous Mesoporous Mater 86:277–286

Nadaroglu H, Kalkan E, Demir N (2010) Removal of copper from aqueous solution using red mud. Desalination 251:90–95

Ozsoy D, Kumbur H (2006) Adsorption of Cu(II) ions on cotton boll H. J Hazard Mater B136:911–916

Pinto MVS, Silva DL, Saraiva ACF (2012) Obtenção e caracterização de carvão ativado de caroço de buriti (*Mauritia flexuosa L. f.*) para a avaliação do processo de adsorção de cobre(II). Acta Amazônica 42:73–80

Santona L, Castaldi P, Melis P (2006) Evaluation of the interaction mechanisms between red muds and heavy metals. J Hazard Mater B136:324–329

Sarıa A, Tuzena M, Cıtaka D, Soylakb M (2007) Adsorption characteristics of Cu(II) and Pb(II) onto expanded perlite from aqueous solution. J Hazard Mater 148:387–394

Tito GA, Chaves LHG, Ribeiro S, Souza RS (2008) Isotermas de adsorção de cobre por bentonita. Rev Caatinga 21:16–21

Valentini A, Laranjeira MCM, Fiori S, Fávere VT (2000) Processo alternativo para remoção de cobre(II) e níquel(II) de soluções aquosas utilizando cápsulas de quitosana-álcool polivinílico. Quim Nova 23:12–15

Valladares GS, Pereira MG, Alves GC (1998) Aplicação de duas isotermas de adsorção de boro em solos de baixada do estado do Rio de Janeiro. Rev Bras Ciênc Solo 22:361–365

Von Sperling M (2005) Introdução à qualidade das águas e ao tratamento de esgotos, 3rd edn. UFMG, Belo Horizonte

Zhua Y, Hua J, Wanga J (2012) Competitive adsorption of Pb(II), Cu(II) and Zn(II) onto xanthate-modified magnetic chitosan. J Hazard Mater 221–222:155–161